Bulletin of the Seismological Society of America, Vol. 82, No. 2, pp. 1124–1133, April 1992

SHORT NOTES

EFFECTS OF AN ALLUVIAL BASIN ON STRONG GROUND MOTIONS

BY KUO-LIANG WEN, YEONG TEIN YEH, AND WEN-GEE HUANG

It has been reported that structures on loose soil sustain more damage during earthquakes than those on solid rock. This phenomenon has long been ascribed to the influence of local site geology. Gutenberg (1956) observed stronger shaking and longer duration at sites on alluvium than at those on crystalline rock, and large variations in ground shaking even at sites only 1000 feet apart. During the recent Michoacań earthquake of 1985, most of the damages occurred in Mexico City more than 300 km from the epicenter (Anderson *et al.*, 1986). The city is situated atop very soft sediments that caused dramatic amplification of strong ground motion, severe damage to the structures, and considerable loss of life within the area of the city located on top of the soft sediments.

On 20 May 1986 a magnitude $M_L = 6.5$ earthquake occurred near Hualien in eastern Taiwan. The epicenter was located at 24°4.9′N and 121°35.49′ E, and the focal depth was 15.8 km. This earthquake caused some damage in the Hualien and Taipei areas (Tsai *et al.*, 1986). Accelerographs at 37 sites of the Strong Motion Accelerographs Array in Taiwan phase 1 (SMART1 array, Fig. 1; Bolt *et al.*, 1982) were triggered. The Lotung Large Scale Seismic Test Array (LSST Array, Figs. 1 and 2; Wen *et al.*, 1986) is situated within the southwestern quadrant of the SMART1 array. Surface recordings and two groups of downhole recordings of the LSST array were also obtained. In this study, we use the frequency-wavenumber (f-k) analysis to study the variations in wave propagation direction and velocity. The change in peak acceleration, velocity, and displacement with respect to depth and the frequency-dependent ground motion amplification are studied by using the downhole and surface recordings of the LSST array.

THE SMART1 ARRAY DATA

From the SMART1 array center (C00), the epicentral distance and azimuth of the Hualien earthquake are 68 km and 195°, respectively. Figure 3 is an illustration of some horizontal accelerograms recorded by the SMART1 array. In this figure, the time traces are plotted in a form commonly used with exploration geophone spreads. Because absolute time is available, the records can be correlated against epicentral distances in real time. Note the coherent S pulses on the horizontal components can be seen clearly across the whole array.

Figure 4 is the contour map of peak ground accelerations for the EW component in the SMART1 array area caused by this earthquake. The contour interval is 10 gals. The symbols "+" and "−" in the map represent the contour high and low, respectively. The largest peak acceleration is about 0.21 g and it occurred near stations O04, O05, and M06; the lowest peak acceleration is about 0.09 g and it occurred near station O12. The differences in maximum acceleration can be as much as 0.13 g within an area of 12 km^2. This large variation over a distance of less than 4 km accentuates the difficulty in describing an

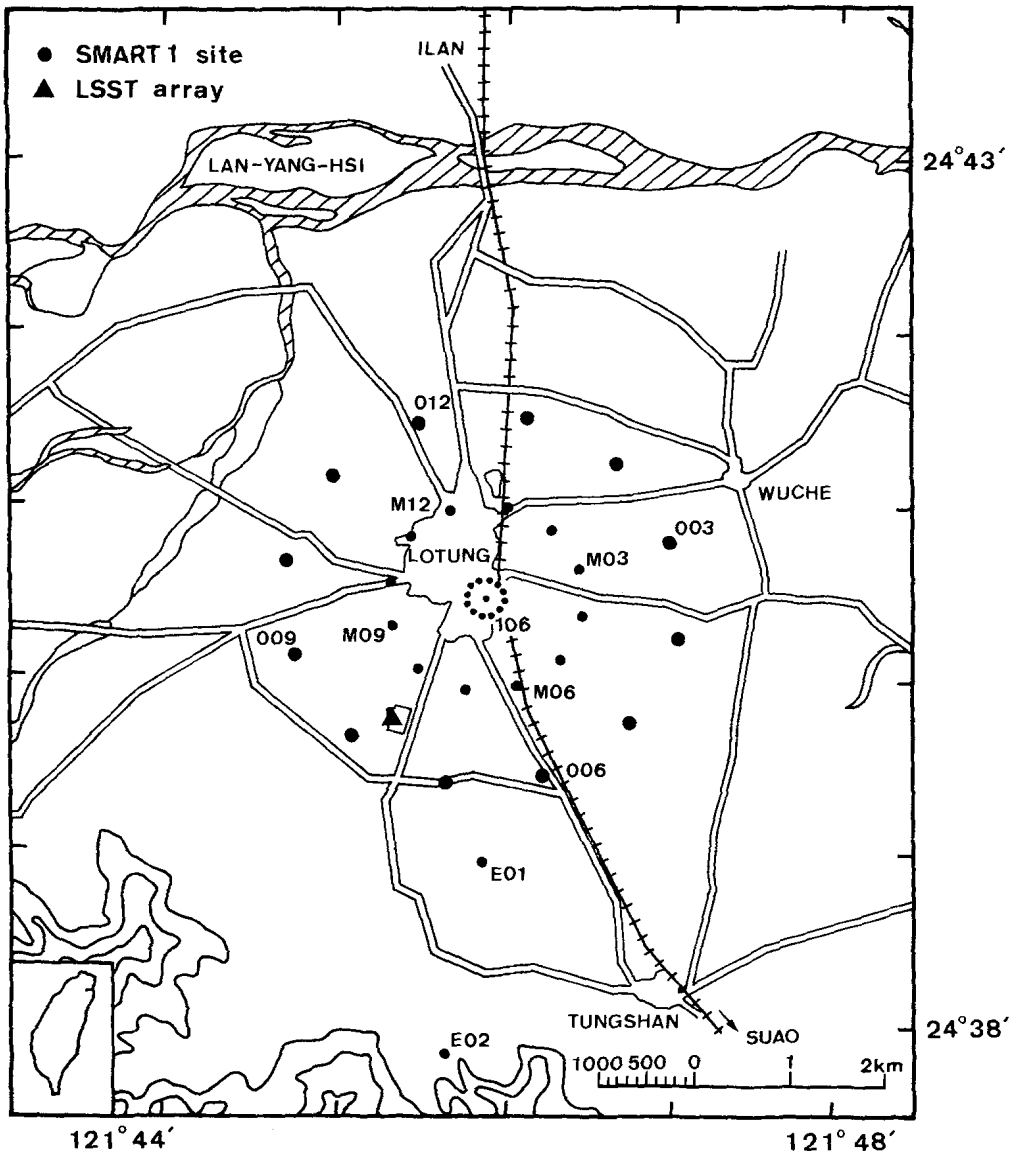

FIG. 1. Layout of the SMART1 array.

accelerogram simply by its peak value. The reasons for these differences may be the differences of the local site geology or the properties of the subjacent strata.

f-k ANALYSIS

Using the algorithm of Capon (1969), the *f-k* spectrum was computed at a discrete frequency as a function of wavenumber k and was decomposed into two orthogonal components. A 5-sec time window of the S wave (shown in Fig. 3) for the recordings of C00, M-ring, and O-ring (Fig. 1) was used. The *f-k* analysis was conducted on the frequency band of 0.6 to 1.4 Hz, for both EW and NS components. The results from the NS component show that within the 95% confidence interval the wave propagated across the array with an apparent

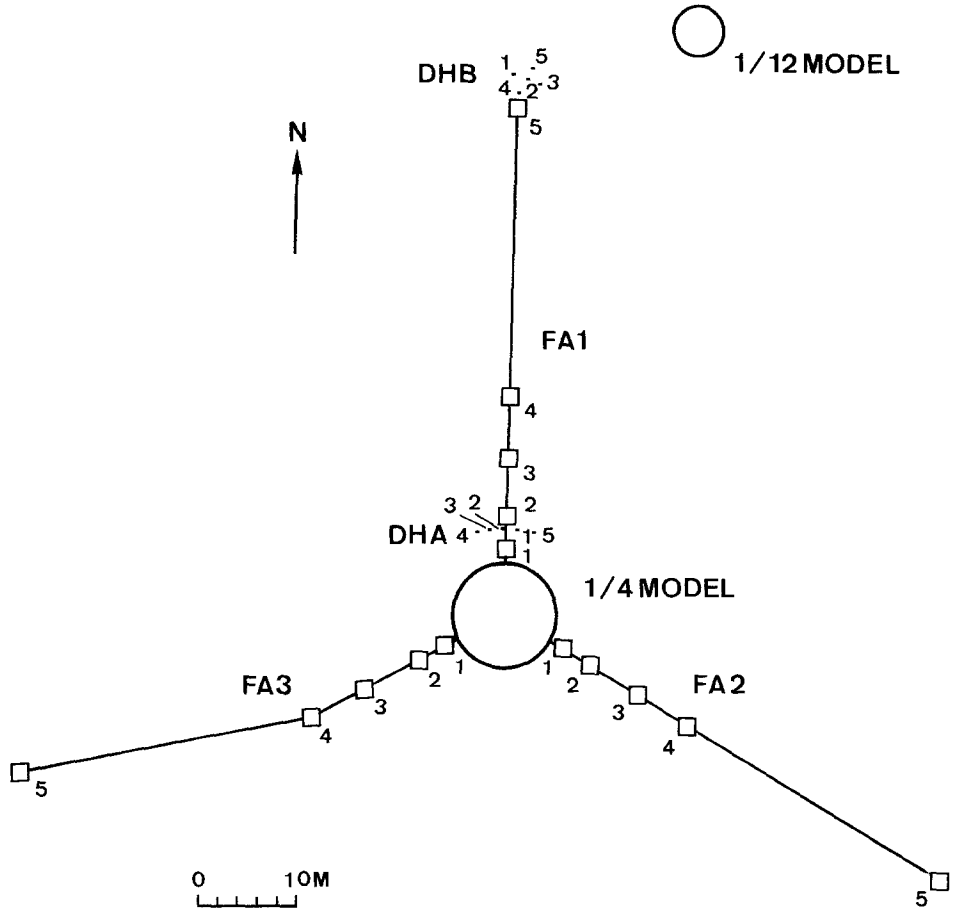

FIG. 2a. The surface instrumentation of the LSST array.

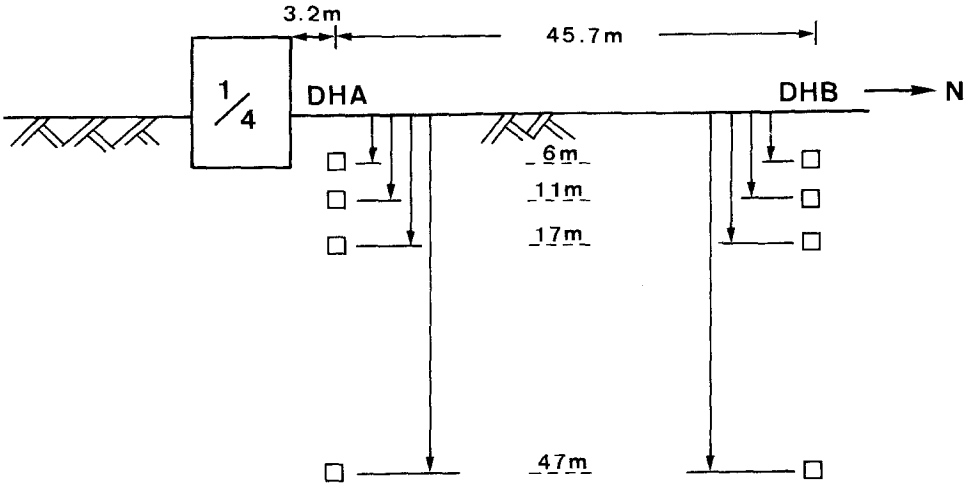

FIG. 2b. The downhole instrumentation of the LSST array.

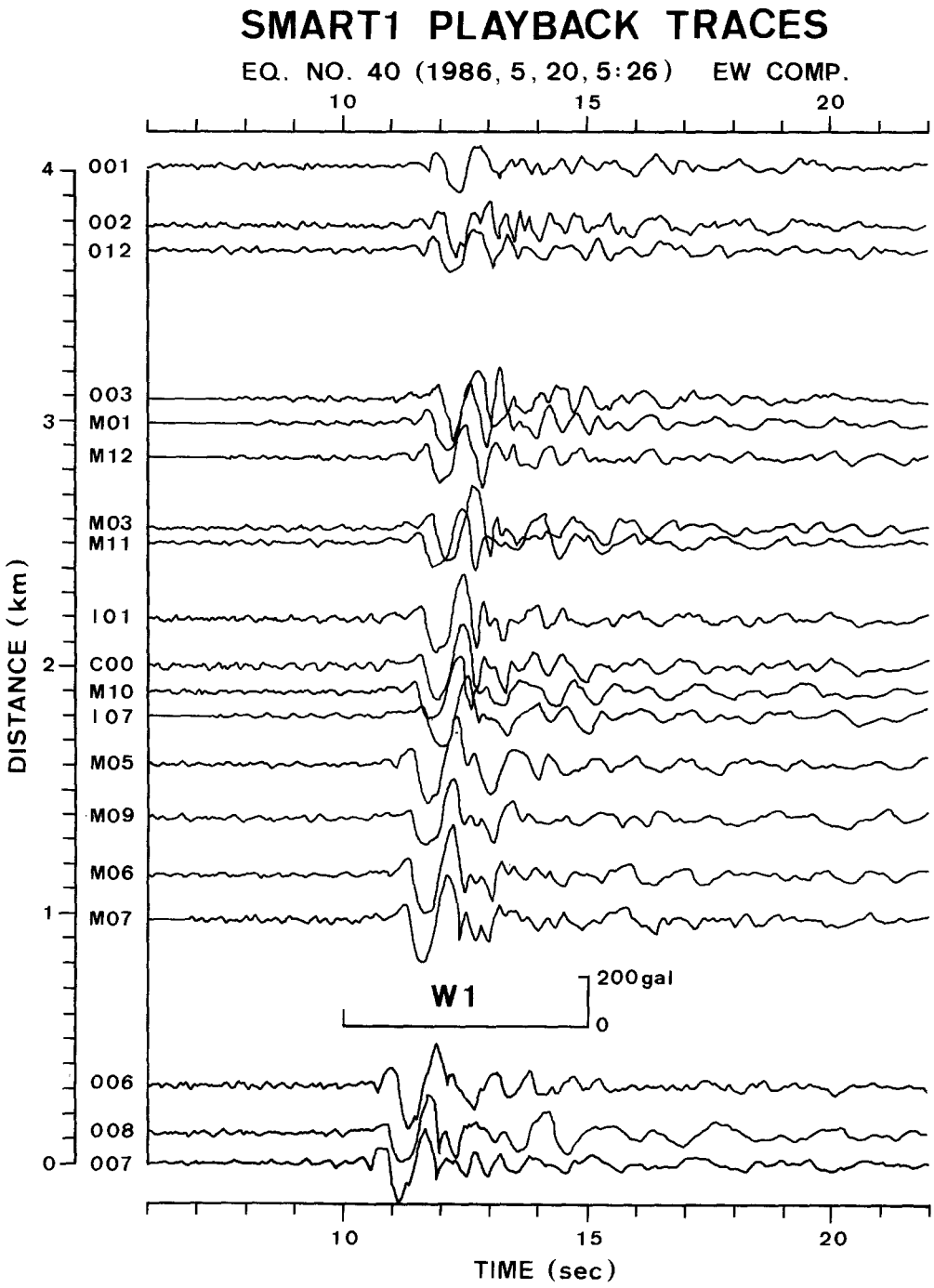

FIG. 3. Acceleration waveforms of EW component recorded at the SMART1 array. The records are aligned in absolute time and are plotted according to increasing epicentral distance. The time window W1 is used for the *f-k* analysis.

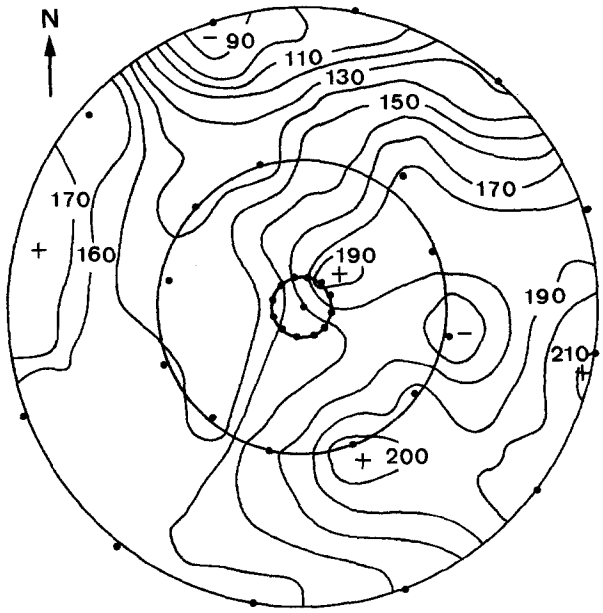

FIG. 4. Contour map of peak acceleration of EW component in the SMART1 array area. The contour interval is 10 gals.

velocity of 3.1 ± 0.5 km/sec and azimuth of S17° ± 7°W. For the EW component, the results are 3.5 ± 0.4 km/sec and S19° ± 7°W. The epicentral azimuth (S15°W) is within the 95% confidence interval of the calculated *S*-wave propagation direction (S10° to S26°W). This indicates that the *S* wave does propagate along the path connecting the focus and the array.

f-k analysis was also performed by using four subarrays, defined by the principal quadrants, in the same frequency range and time window. The wave propagation direction and apparent velocity in each quadrant, calculated from the EW component, for the frequency band of 0.6 to 1.4 Hz are given in Figure 5, and the 95% confidence intervals of velocity and azimuth are also shown in Figure 5 with an error ellipse. It is clear that the mean wave propagation direction in the northern array area was pointed to the NE and the apparent velocity varied from 2.5 km/sec in the southern area to greater than 4.0 km/sec in the northern area. The analyses of the 29 January 1981 Suao earthquake by Bolt *et al.* (1984) also point out the significant change in wave propagation direction occurring over a short distance with significant rotational motion present. This rotational motion suggests the existence of geometrical focusing effects in a three-dimensional basin. These focusing effects and three-dimensional caustics are highly developed by the spherical geometry of the circular basin model considered as shown in the numerical study by Lee and Langston (1983). The basin center of the Lanyang plain is the northeast of the array, and this may explain why the wave path turned to the northeast.

DOWNHOLE RECORDINGS OF THE LSST ARRAY

The decrease of peak horizontal acceleration, velocity, and displacement with increasing depth was studied using the DHB group (see Fig. 2) of downhole recordings of the LSST array. The maximum of the two horizontal peak

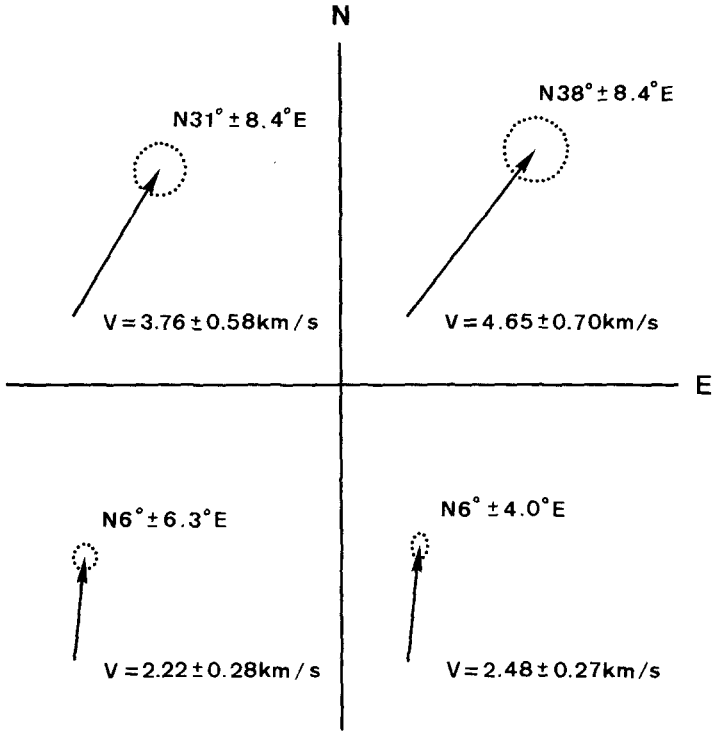

FIG. 5. Average wave propagation direction and apparent velocity of S wave in the frequency band of 0.6 to 1.4 Hz as calculated from EW component. The 95% confidence interval is shown by an error ellipse.

accelerations, velocities, and displacements were designated as the PGA, PGV, and PGD, respectively. To understand the relationships between the peak amplitudes and depth, the peak amplitudes recorded at the downhole sites were normalized with respect to the surface sites and shown in Figure 6. Using linear regression analysis, we obtain the empirical relationships between the normalized parameters, NPGA, NPGV, and NPGD, and depth. The relationships are as follows:

$$NPGA = e^{-0.1827H^{0.4068}},$$
$$NPGV = e^{-0.0108H^{1.2346}},$$
$$NPGD = e^{-0.0026H^{1.5063}},$$

where H is depth in m. These equations are plotted as dashed lines in Figure 6. The PGAs at the surface are about 2.1 times greater than those at 47-m depth. This ratio agrees with the results in the Richmond area in California, where the PGA at the free surface is about 1.6 to 2.8 times greater than that at 40-m depth (Johnson and Silva, 1981). The shear wave velocity at Richmond between 0 and 36 m depth is about 100 to 300 m/sec (Johnson and Silva, 1981), which is similar to that under the LSST array (Vs = 120–280 m/sec in the upper 50 m soil; Wen and Yeh, 1984; HCK, 1986).

The effects of a soil layer can be examined by comparing the Fourier spectrum of an alluvium site to that of a rock site or of a surface site to that of a downhole

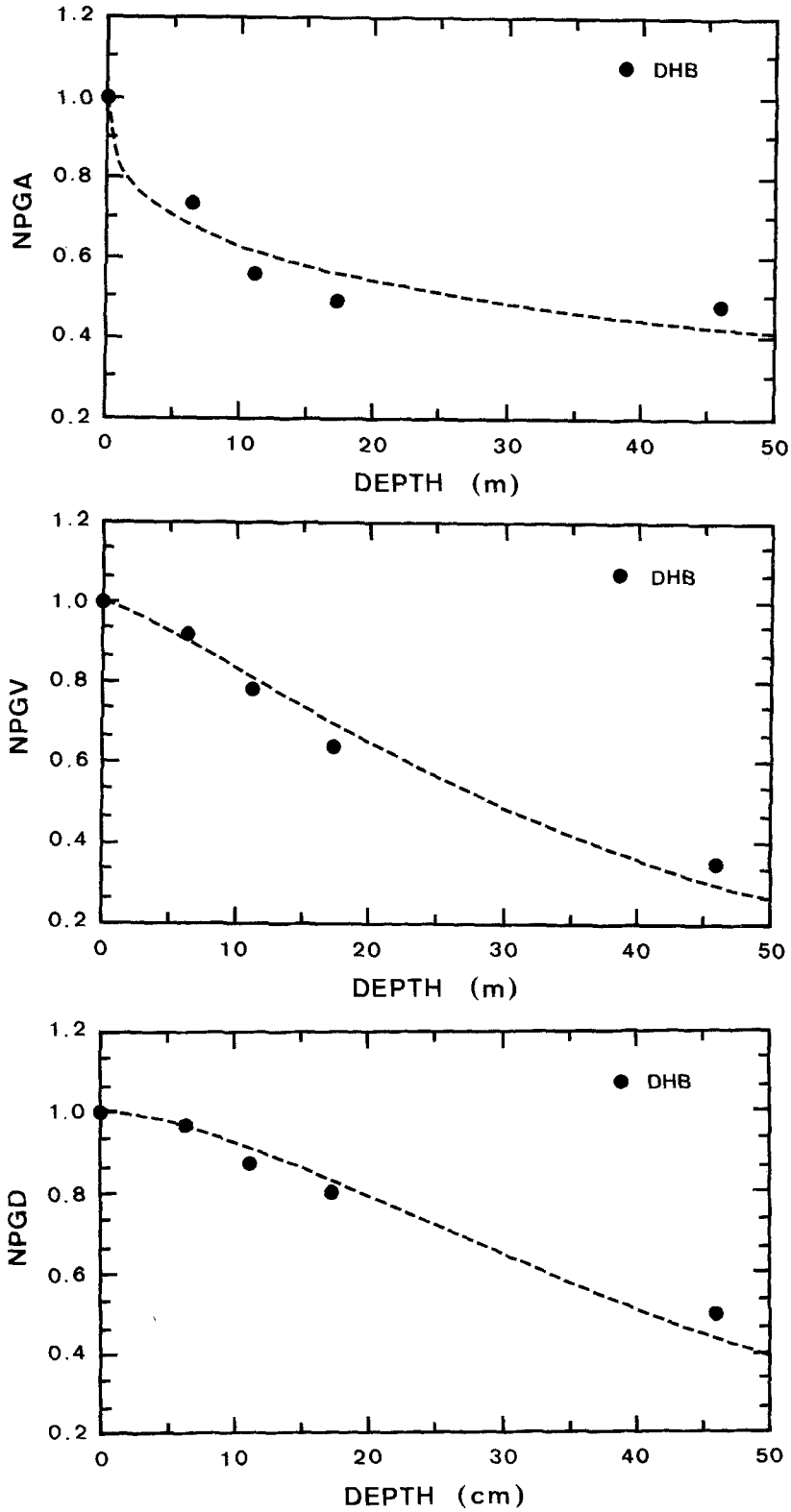

FIG. 6. Variations of the normalized peak ground motions with respect to depth in the LSST array. (a) Acceleration, NPGA; (b) velocity, NPGV; and (c) displacement, NPGD.

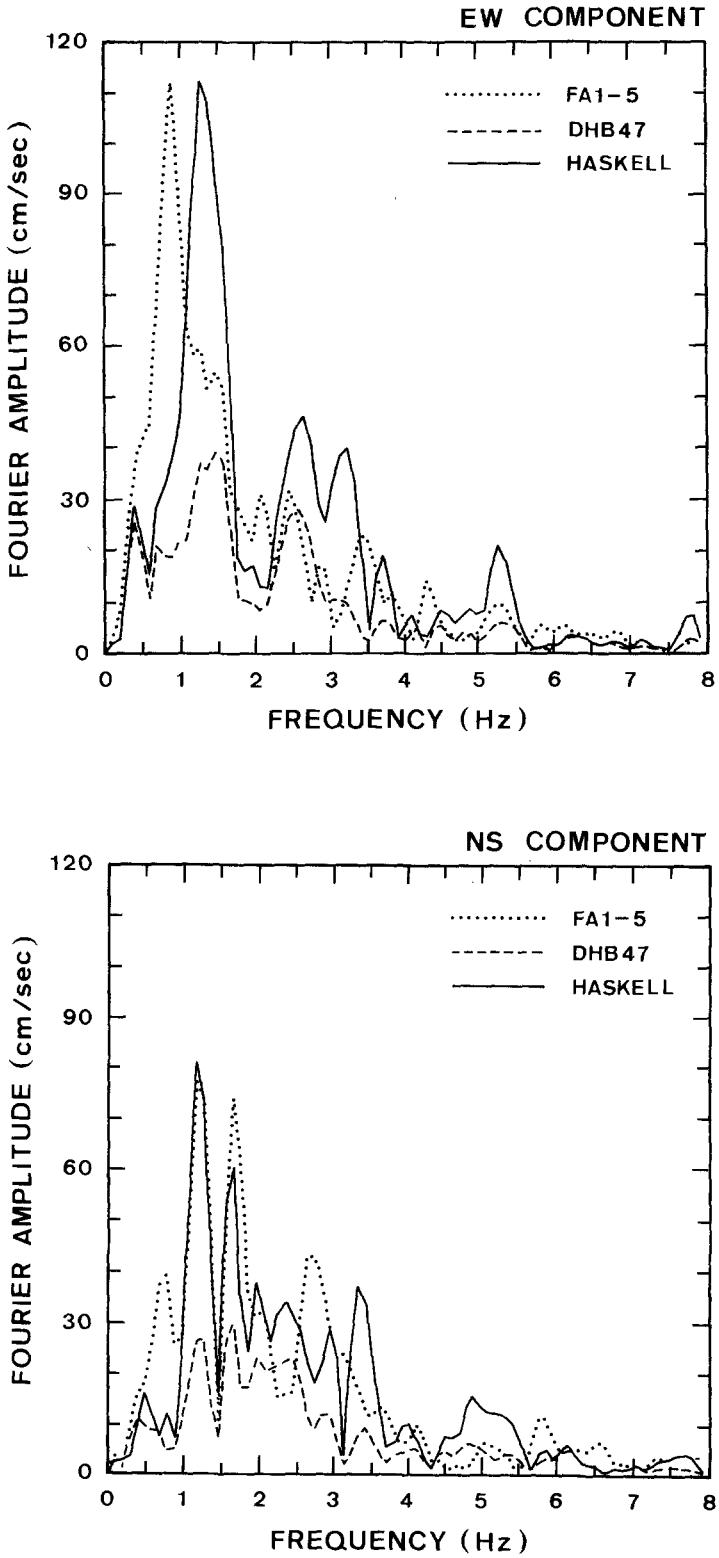

FIG. 7. The Fourier spectra of surface and DHB47 downhole recordings. The solid line show the results estimated by using the record of DHB47 as input.

site. In our study, the first 5.12 sec signals after the S arrival is extracted from the original accelerogram by a tapered box-car window to calculate the Fourier spectrum. The Fourier spectra of the FA1-5 surface and the DHB47 downhole recordings are compared. The frequency band in which the ground motion has been amplified by the sedimentary layer is shown in Figure 7. The soil amplification effect is significant in the frequency band of 0.5 to 2.0 Hz. The dominant frequencies are about 0.9 and 1.3 Hz, respectively, for the EW and NS components. According to the velocity-depth profile at the site (Wen and Yeh, 1984; HCK, 1986), the downhole accelerographs are located in the top two sedimentary layers with thicknesses of 10 and 40 m and S-wave velocities of 120 to 160 and 190 to 280 m/sec, respectively. We use the average velocity model of 140 and 250 m/sec for these two layers (assume constant Q equal to 10) and the record of DHB47 as input. Based on Haskell's method (1960), we can see that the estimation (shown on Fig. 7) of the NS component fits the observations well. However, the estimation of the EW component shows a shift of the peak frequency from 0.9 to 1.25 Hz. The downhole recordings of this earthquake were analyzed for evidence of nonlinear soil response during strong shaking (Chang *et al.*, 1989). Effective shear moduli or shear-wave velocities decreased as the level of shaking increased. For the soil layer between 11 and 17 m, the effective shear wave velocities were 81 and 145 m/sec, respectively, for EW and NS components (Chang *et al.*, 1989). The shear-wave velocity from *in situ* geophysical measurements is 187 m/sec. This may explain why the soil responses of the EW and NS components are different.

Acknowledgments

This work was supported by the National Science Council and the Institute of Earth Sciences, Academia Sinica. The LSST array is funded by the Taiwan Power Company (R.O.C.) and the Electrical Power Research Institute. Discussions with B. S. Huang, G. B. Ou, and B. Y. Kuo are greatly appreciated. The authors thank Dr. C. B. Crouse and an anonymous reviewer for their constructive comments and suggestions.

References

Anderson, J. G., P. Bodin, J. N. Brune, J. Prince, S. K. Singh, R. Quaas, and M. Oñate (1986). Strong ground motion from the Michoacan, Mexico, earthquake, *Science* **233**, 1043–1049.

Bolt, B. A., N. A. Abrahamson, and Y. T. Yeh (1984). The variation of strong ground motion over short distance, in *Proc. 8th World Conf. Earthq. Eng.*, San Francisco.

Bolt, B. A., C. H. Loh, J. Penzien, Y. B. Tsai, and Y. T. Yeh (1982). Preliminary report on the SMART1 strong motion array in Taiwan, EERC Report No. UCB/EERC-82/13.

Capon, J. (1969). High resolution frequency-wavenumber spectrum analysis, *Proc. IEEE* **57**, 1408–1418.

Chang, C. Y., M. S. Power, Y. K. Tang, and C. M. Mok (1989). Evidence of nonlinear soil response during a moderate earthquake, in *Proc. 12th Int. Conf. Soil Mech. and Foundation Eng.*, Brazil.

Gutenberg, B. (1956). Effects of ground on earthquake motion, *EOS* **37**, 757–760.

Haskell, N. A. (1960). Crustal reflection of plane SH waves, *J. Geophys. Res.* **65**, 4147–4150.

HCK (1986). Geophysical survey report of Lo-Tung project for Taiwan Power Company, HCK Geophysical Company.

Johnson, L. R. and W. Silva (1981). The effects of unconsolidated sediments upon the ground motion during local earthquakes, *Bull. Seism. Soc. Am.* **71**, 127–142.

Lee, J. J. and C. A. Langston (1983). Wave propagation in a three-dimensional circular basin, *Bull. Seism. Soc. Am.* **73**, 1637–1653.

Tsai, C. C., Y. T. Yeh, K. L. Wen, S. N. Cheng, and M. H. Kao (1986). The Hualien earthquake of May 20, 1986: Strong ground motion data and response spectra, *Bull. Inst. Earth Sci., Academia Sinica* **6**, 29–64.

Wen, K. L. and Y. T. Yeh (1984). Seismic velocity structure beneath the SMART1 array, *Bull. Inst. Earth Sci., Academia Sinica* **4**, 51–72.

Wen, K. L., Y. T. Yeh, and C. C. Liu (1986). The observation system and data processing of the LSST array, Institute of Earth Sciences, Academica Sinica, ASIES-CR8602, (in Chinese).

INSTITUTE OF EARTH SCIENCES
ACADEMIA SINICA
P. O. BOX 23-59
TAIPEI, TAIWAN 10764
REPUBLIC OF CHINA

Manuscript received 6 March 1990